

Supporting Information

Polymeric Cobalt(II) Thiolato Complexes — Syntheses, Structures and Properties of ∞ [Co(SMes)₂] and ∞ [Co(SPh)₂NH₃].

Andreas Eichhöfer,^{*,abc} Gernot Buth^d

^a Institut für Nanotechnologie, Karlsruher Institut für Technologie (KIT), Campus Nord,

Hermann-von-Helmholtz-Platz 1, 76344 Eggenstein-Leopoldshafen, Germany

Tel. 49-(0)721-608-26371

Fax: 49-(0)721-608-26368

e-mail: andreas.eichhoefer@kit.edu

^b Lehn Institute of Functional Materials, Sun Yat-Sen University, Guangzhou 510275, China

^c Karlsruhe Nano Micro Facility (KNMF), Hermann-von-Helmholtz-Platz 1, 76344

Eggenstein-Leopoldshafen, Germany

^d Institut für Photonenforschung und Synchrotronstrahlung, Karlsruher Institut für

Technologie (KIT), Campus Nord, Hermann-von-Helmholtz-Platz 1, 76344 Eggenstein-

Leopoldshafen, Germany

Content

Figure S1 Measured and simulated X-ray powder pattern of **1**.

Figure S2 Shortest intermolecular interactions in the crystal structure of **3**.

Figure S3 – S5 Measured and simulated X-ray powder pattern for **2 – 4**.

Figure S6 Plot of the magnetization M versus T for **2** at 4K.

Figure S7 Plots of the reduced magnetization M versus H/T for **3**.

Figure S8 Plot of the magnetization M versus T for **4** at 4K.

Figure S9 Thermogravimetric analysis of **3** under helium gas flow and in vacuum.

Figure S10 X-ray powder pattern of the vacuum TGA product of **4**.

Figure S11 X-ray powder patterns of intermediate TGA products of **4**.

List of compounds

$\text{[Co(SPh)}_2\text{] (1)}$

$\text{[Co(SMes)}_2\text{] (2)}$.

$\text{[Co(SPh)}_2\text{(NH}_3\text{)}_2\text{] (3)}$.

$\text{[Co(SPh)}_2\text{(NH}_3\text{)] (4)}$.

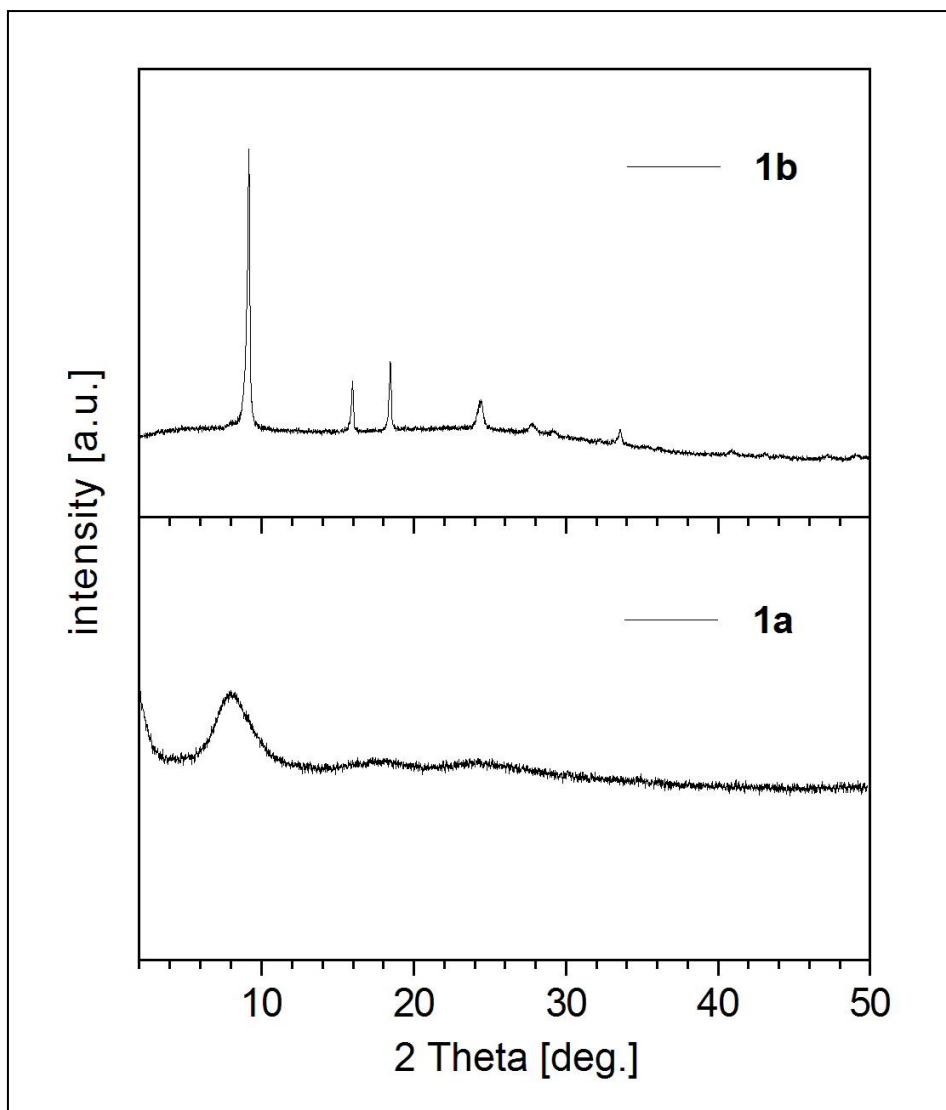


Figure S1 X-ray powder pattern for $\text{Co}(\text{SPh})_2$ (**1**) synthesized at rt (**1a**) and at 105 °C (**1b**).

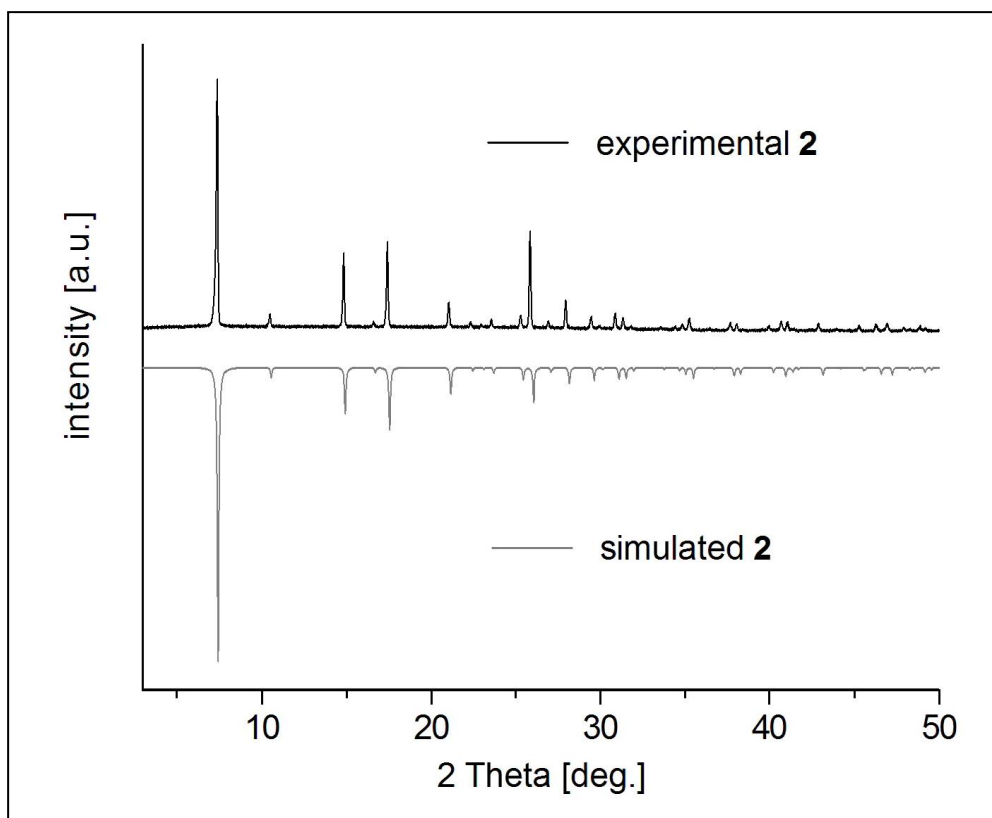


Figure S3 Measured (black) and simulated (grey) X-ray powder patterns for $\infty[\text{Co}(\text{SMes})_2]$.

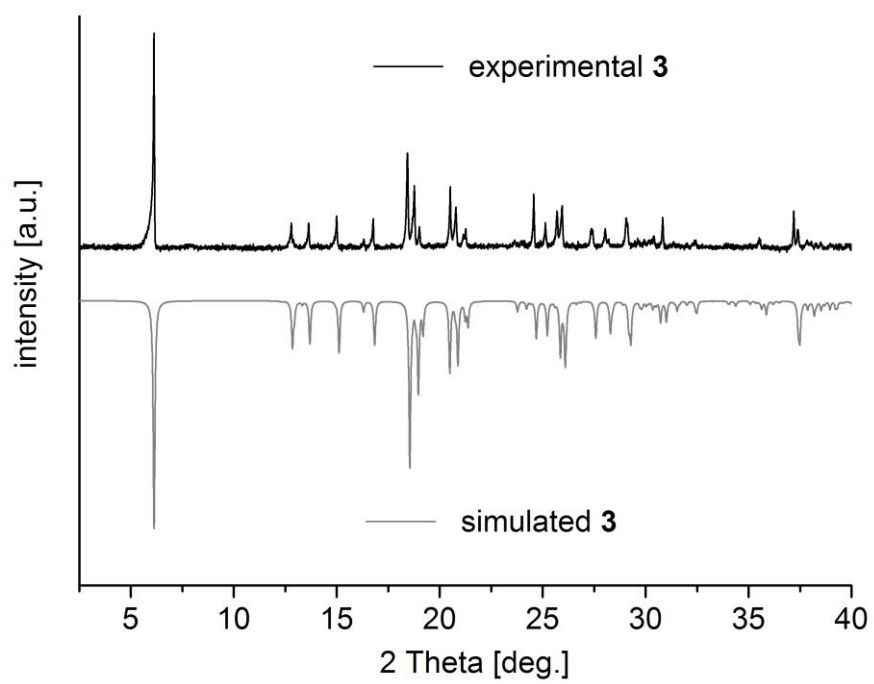


Figure S4 Measured (black) and simulated (grey) X-ray powder patterns for [Co(SPh)₂(NH₃)₂] (**3**).

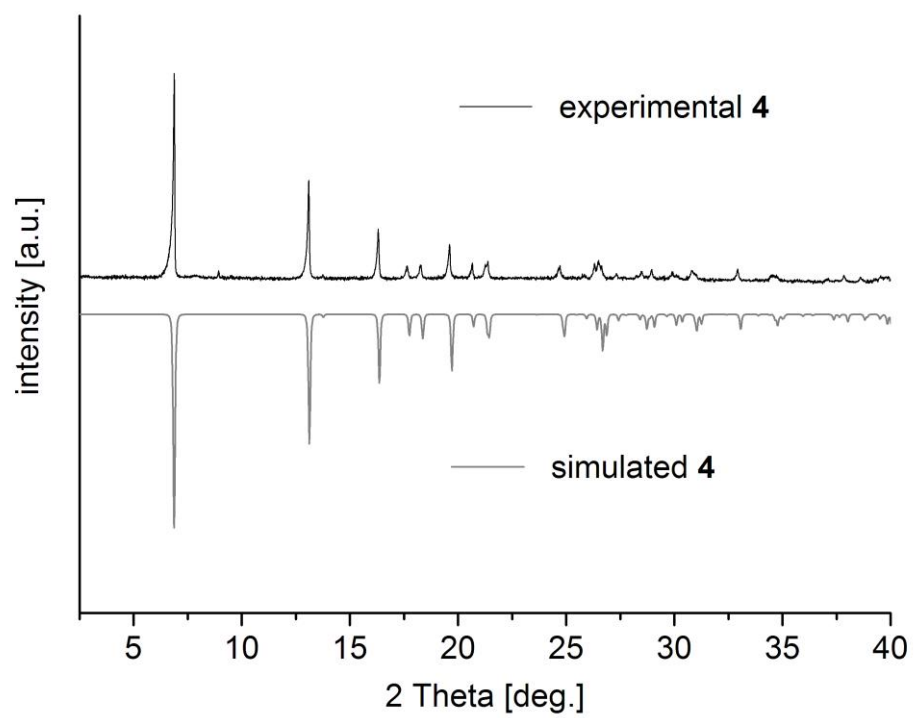


Figure S5 Measured (black) and simulated (grey) X-ray powder patterns for $\infty^1[\text{Co}(\text{SPh})_2(\text{NH}_3)]$ (**4**).

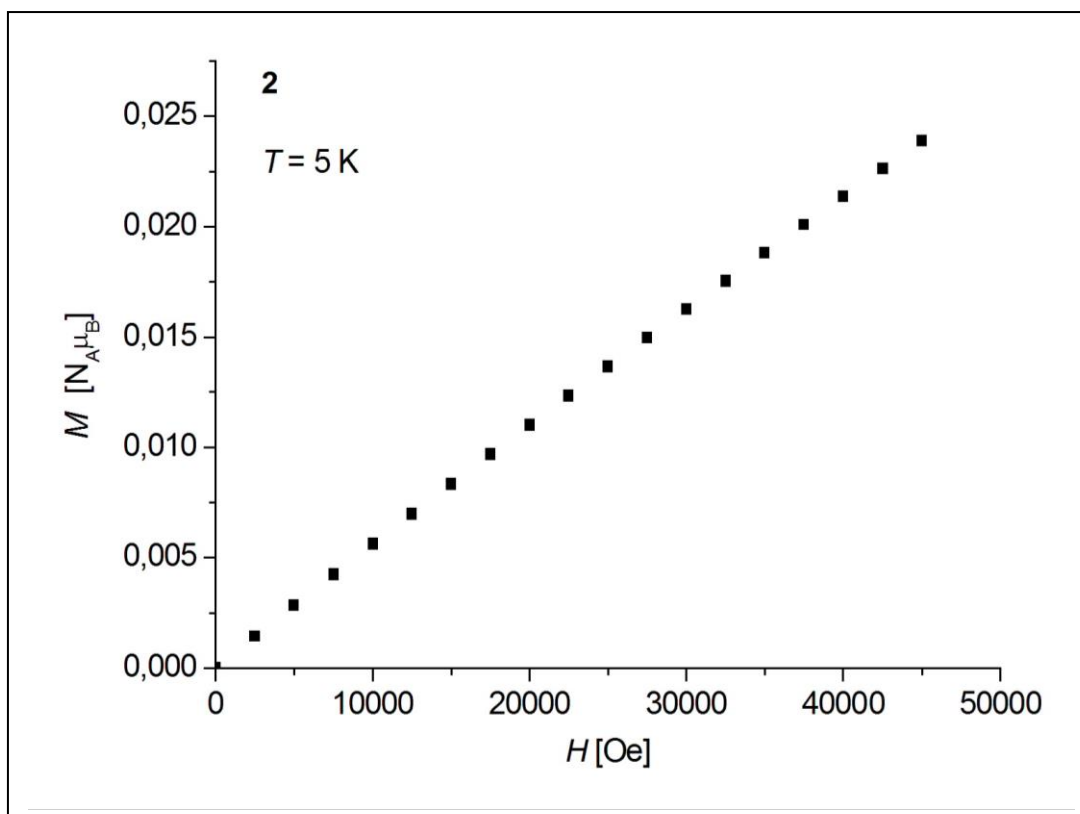


Figure S6 Plot of the magnetization M versus T for $\frac{1}{\infty}[\text{Co}(\text{SMes})_2]$ (**2**) at 5K.

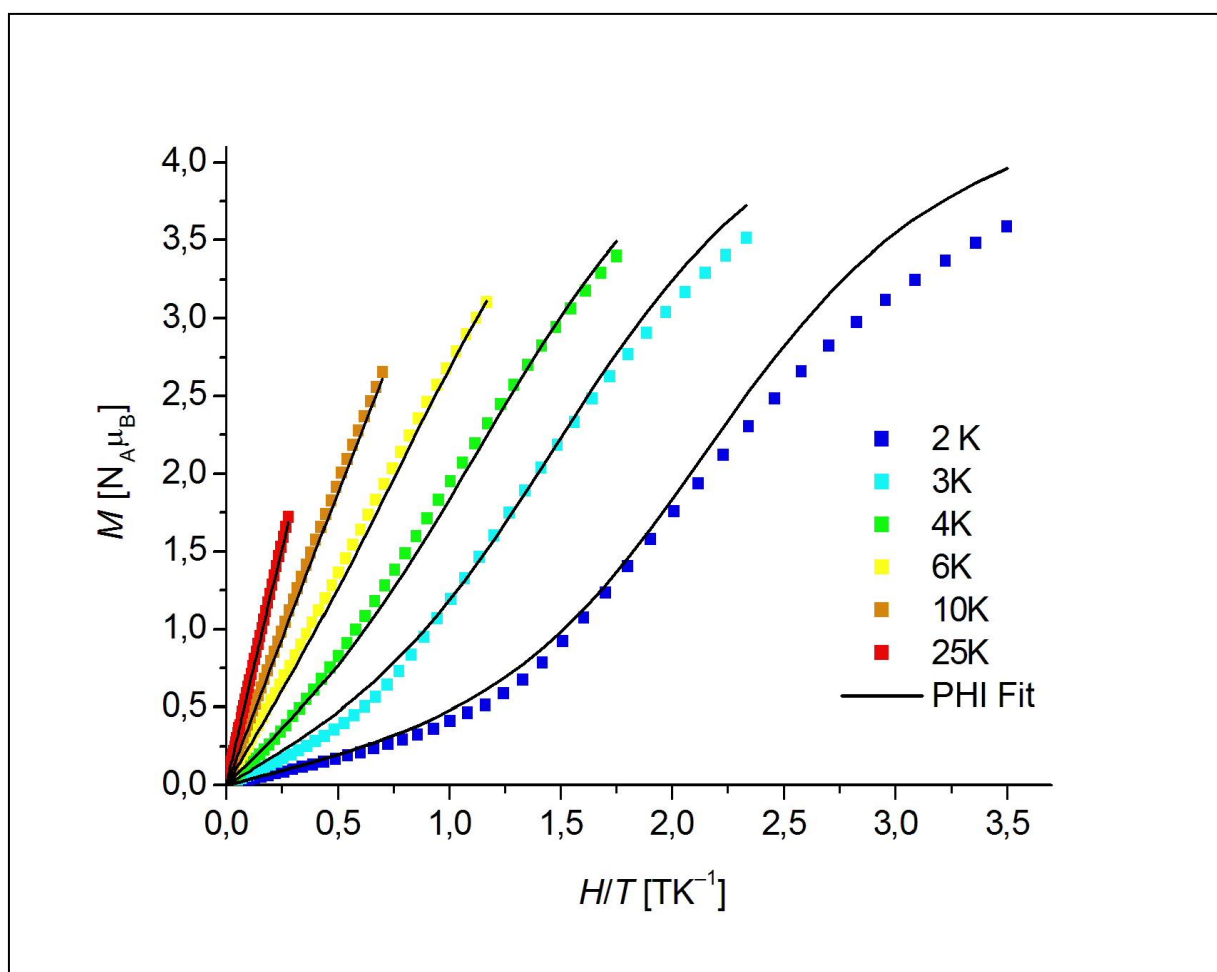


Figure S7 Plots of the reduced magnetization M versus H/T for $[\text{Co}(\text{SPh})_2(\text{NH}_3)_2]$ (**3**) at different temperatures. The solid lines represent the calculated curves (eqn (1)) with the PHI program.¹

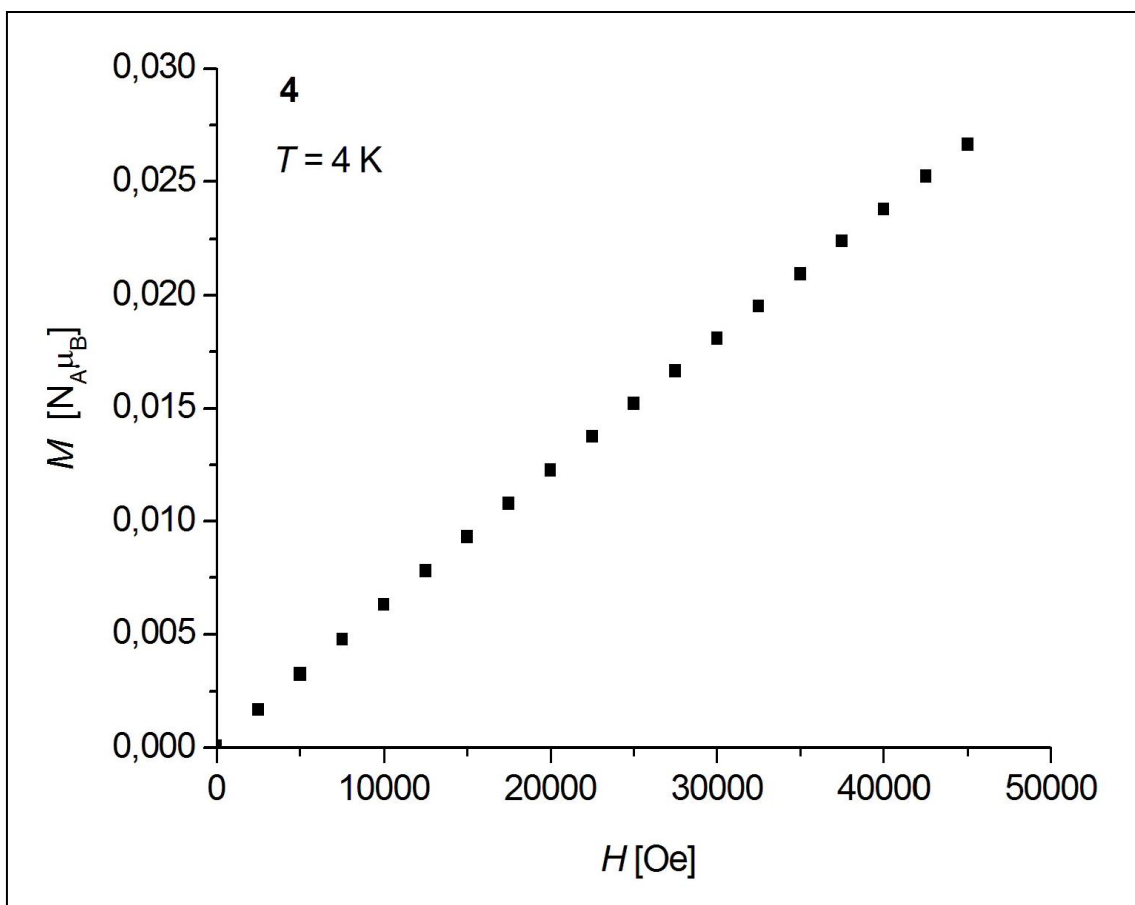


Figure S8 Plot of the magnetization M versus T for ∞ [$\text{Co}(\text{SPh})_2(\text{NH}_3)$] (**4**) at 4K.

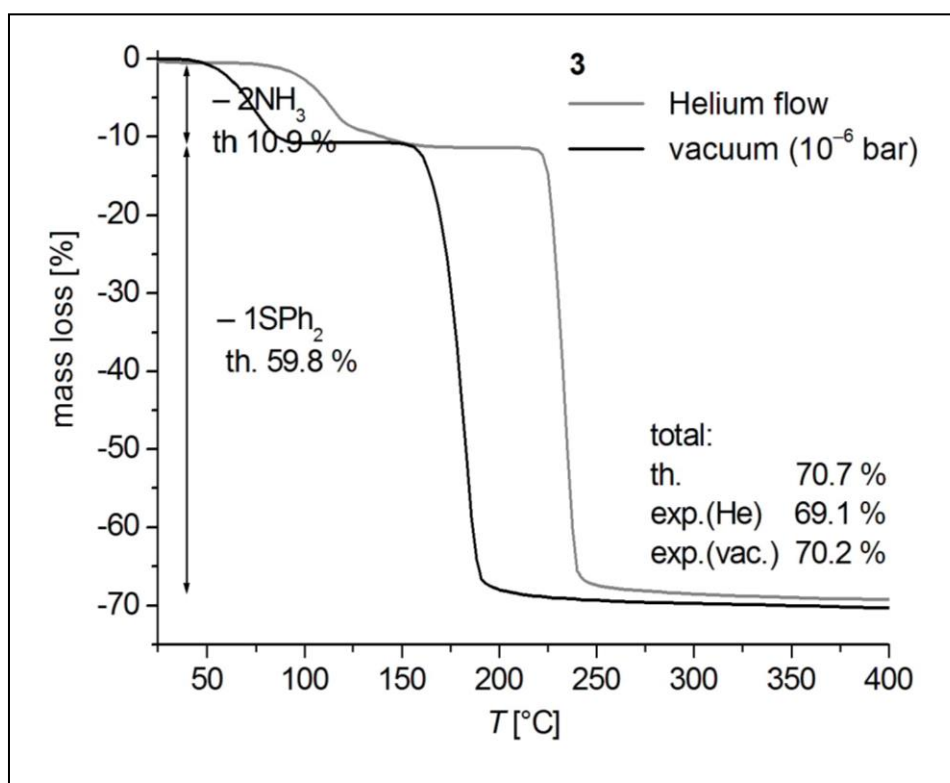


Figure S9 Thermogravimetric analysis of $[\text{Co}(\text{SPh})_2(\text{NH}_3)_2]$ (**3**) under helium gas flow and in vacuum.

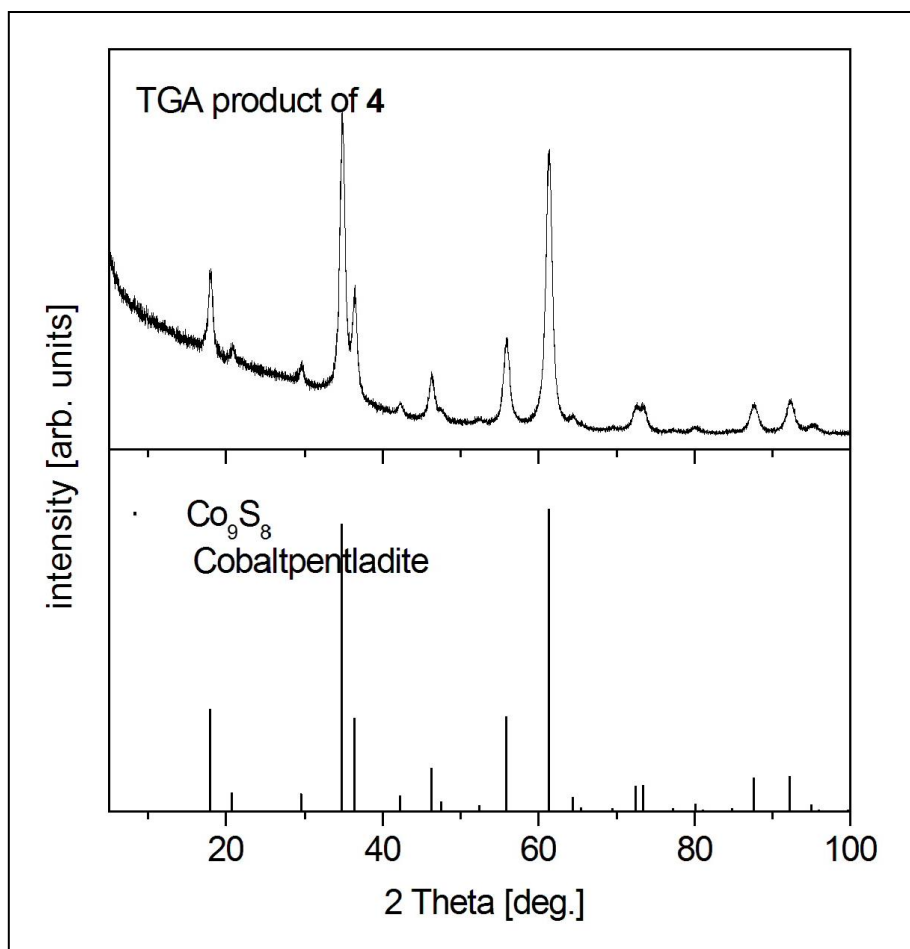


Figure S10 X-ray powder pattern of the vacuum TGA product of $\frac{1}{\infty}[\text{Co}(\text{SPh})_2(\text{NH}_3)]$ (**4**) heated to 555 °C compared to the theoretical peak pattern of the cobalt pentlandite structure from ref (1).

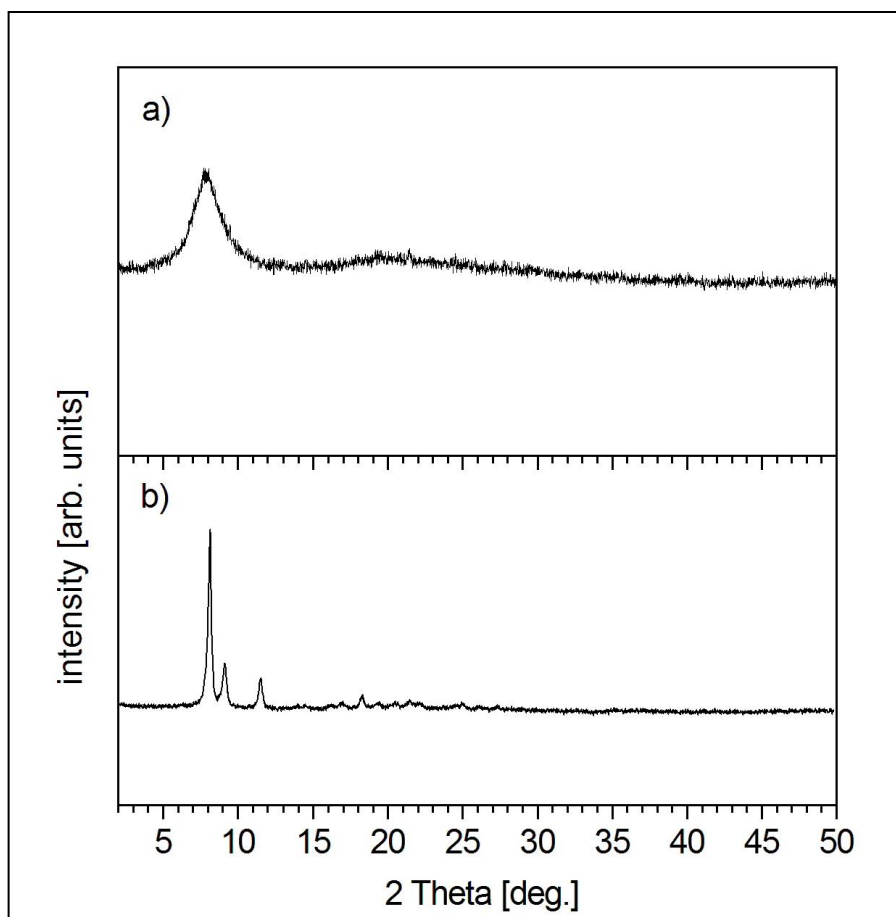


Figure S11 X-ray powder pattern of intermediate TGA products of $\infty^1[\text{Co}(\text{SPh})_2(\text{NH}_3)]$
(4) a) heated to 110°C under vacuum (2K/min) and isothermal treatment for 1 hour b)
same residue post-annealed under N_2 at 150°C for 3 – 4 h..